UNIABUJA Journal of Engineering and Technology

https://ujet.uniabuja.edu.ng/

Special Issue

Design and Implementation of Smart Radiation Monitoring Device

Kazeem Adetunji SODIQ[1*], Ernest King ADEWOLE[2], Olukayode Samson OLOPADE[3], Hamzat Babajide OJO[4], Lateef Abolanle SALIU[5], Solomon SALAU[6], Latifat Folake ODERINU[7], Oyesola Oluwasesan AWOYOOLA[8]

[1,2,3,5,6,7] *Department of Computer Engineering, Yaba College of Technology Lagos, Nigeria*

[4] *Department of Electrical/Electronic Engineering, Federal University of Technology, Ilaro, Ogun State*

[8] *Department of Computer Technology, Yaba College of Technology Lagos, Nigeria*

[1*]kazeem23@yahoo.com, adewoleernest@gmail.com, olukayode.olopade@yabatech.edu.ng, babajide.ojo@federalpolyilaro.edu.ng, lateef.saliu@yabatech.edu.ng, solomonsalau89@gmail.com, latifat.oderinu@yabatech.edu.ng, oyesola.awoyoola@yabatech.edu.ng

Abstract

This research presents the design and implementation of a Smart Radiation Monitoring Device aimed at providing real-time, affordable, and portable detection of ionizing radiation, with integrated cloud-based data logging. The device utilizes a Geiger-Müller tube for sensing environmental radiation, a NodeMCU (ESP8266) microcontroller for processing and Wi-Fi connectivity, and a 16×2 LCD for real-time visual feedback. Radiation data is uploaded periodically to the ThingSpeak cloud platform, ensuring remote access and historical tracking. The device was tested using naturally occurring low-level radiation sources including granite countertops, ceramic materials, bananas (Potassium-40), and vintage items with trace radioactive content. Measurements recorded ranged from 18–52 counts per minute (CPM), corresponding to dose rates between 0.06–0.21 µSv/hr, all within internationally accepted environmental safety standards. The buzzer functioned as intended, emitting audible clicks with each detected ionizing event, while battery stability supported up to 8 hours of continuous operation without recharge. Experimental results confirm that the system is capable of detecting natural radiation variations accurately and consistently in both indoor and outdoor settings. The project achieved its objective of building a compact and responsive radiation detection system with cloud logging and real-time alert capabilities. Future enhancements may include GSM-based connectivity and GPS-based location tagging to support mobile radiation mapping. Its affordability, ease of use, and real-time monitoring make it suitable for educational use, laboratory safety, environmental surveying, and public health applications.

Keywords: *Geiger–Müller Tube, IoT Cloud Logging, Portable Environmental Dosimetry, Real-Time Radiation Detection, Smart Radiation Monitoring.*

1.0 Introduction

Radiation monitoring is increasingly vital for public safety, healthcare, and industrial operations due to growing exposure risks from medical procedures, nuclear power, and environmental contamination (Andresz et al., 2022). Clinically, staff in interventional radiology face occupational risks (Picano & Vano, 2011; Park et al., 2022), while major incidents such as the Fukushima Daiichi nuclear accident have demonstrated the importance of radiation dose reconstruction, environmental monitoring, and rapid emergency-response systems for protecting public health and supporting recovery efforts (Ohba et al., 2020).

Traditional devices like Geiger counters offer localized readings but lack continuous data logging, remote transmission, and predictive capabilities, limiting their effectiveness in emergencies or distributed environments. High-security applications require sensitive detection near background levels with minimal false alarms (Huang et al., 2024), creating a technological gap for intelligent solutions.

Artificial Intelligence (AI) and Machine Learning (ML) enhance detection accuracy, reduce false positives, and improve response times by analyzing complex radiation patterns (Baek et al., 2021). In radiation oncology, ML improves image contouring, quality assurance, and adaptive planning (Wall et al., 2020; Thwaites et al., 2021). AI in radiomics offers predictive modeling potential, though data harmonization and interpretability remain barriers (Papadimitroulas et al., 2021). In nuclear power, early AI applications emphasized safety and regulatory compliance (Beck & Behera, 1992).

Modern Internet of Things (IoT)-enabled systems integrate distributed sensors, communication networks, and cloud platforms to facilitate real-time data acquisition, transmission, storage, and remote accessibility with cloud platforms for real-time data transmission and remote accessibility (Ahmad et al., 2021; Saleem et

https://doi.org/10.70118/ujet.2026.sp01.10

al., 2023). IoT frameworks support nuclear emergency preparedness (Muhtadan et al., 2020), though interoperability and noisy data persist (Ullo et al., 2020). Advanced sensors include inorganic scintillating microfiber probes with enhanced resolution (Lv et al., 2020), multi-sensor configurations for robustness (Inaba et al., 2020), and artificial neural networks for signal filtering and dose estimation (Szumega et al., 2021).

Unmanned Aerial Vehicle (UAV)-based radiation mapping enables the safe surveying of contaminated or inaccessible areas while minimizing human exposure to potentially hazardous radiation fields (Towler et al., 2012), and mobile systems are critical for emergency response and border security (Marques et al., 2021). Smart ocean monitoring using networked buoys assesses marine contamination in real time (Tran et al., 2021).

Barriers include limited real-time responsiveness in low-cost devices, high operational costs, lack of standardized data-sharing, cybersecurity vulnerabilities, regulatory uncertainties (Papadimitroulas et al., 2021; Ullo et al., 2020), and the need for explainable AI and transparency in high-risk applications (Thwaites et al., 2021).

To address these gaps, this research designs a Smart Radiation Monitoring Device integrating real-time detection, microcontroller processing, local feedback, and cloud logging. Using a Geiger–Müller tube for gamma/X-rays, a NodeMCU microcontroller processes data into counts per minute (CPM) and microSieverts per hour (μSv/hr), provides audible alerts, and transmits data via Wi-Fi to a cloud platform for remote monitoring.

The device emphasizes affordability, portability, and practical deployment in hospitals, laboratories, environmental surveys, and emergencies. By combining IoT connectivity, real-time feedback, and scalable data integration, it bridges traditional tools and intelligent ecosystems for safer, data-driven radiation management

2.0 Materials

2.1 Block Diagram/Conceptual Framework

The system was developed using a four-stage methodology consisting of system design, hardware integration, software development, and experimental validation. During the design stage, a Geiger–Müller tube was selected as the sensing element and interfaced with a NodeMCU ESP8266 microcontroller. The acquired radiation pulses were processed and converted into CPM and equivalent dose-rate values before being displayed locally and transmitted to the cloud platform.

Figure 1 shows the block diagram of a Smart Radiation Monitoring System consisting of a Geiger-Müller tube for detecting ionizing radiation, a high-voltage signal conditioning circuit, a NodeMCU (ESP8266) microcontroller for processing and conversion of radiation data, an LCD display for real-time visualization of readings, a buzzer for audible event-based alerts, Wi-Fi connectivity for cloud data transmission to ThingSpeak, control buttons for powering and resetting the device.

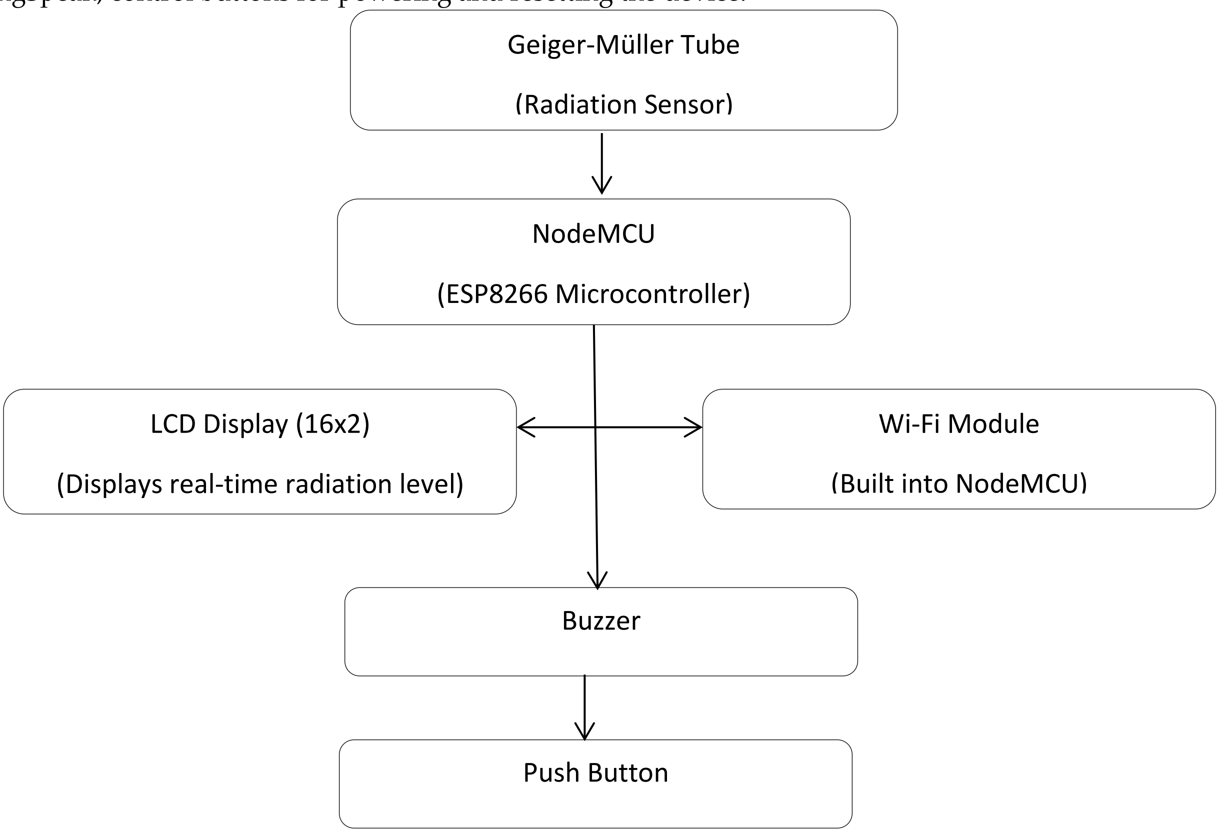

https://doi.org/10.70118/ujet.2026.sp01.10

Figure 1: Block diagram of smart radiation monitoring devices

The Smart Radiation Monitoring Device enables continuous, real-time detection and notification of ionizing radiation by integrating sensing, processing, display, and communication components. A Geiger-Müller (GM) counter detects environmental radiation and generates electrical pulses for each ionizing event, which are processed by a NodeMCU ESP8266 microcontroller. The microcontroller converts raw pulse data from Counts Per Minute (CPM) into standardized microSieverts per hour (µSv/hr), with readings displayed on a 16x2 LCD that updates every second. An audible buzzer provides immediate acoustic feedback for each detected event, mimicking conventional Geiger counters. Data is transmitted wirelessly via Wi-Fi to the ThingSpeak cloud platform for remote access, historical tracking, and trend analysis, with each upload timestamped. User-friendly physical controls, including rocker and push-button switches, allow for device activation, reset, and calibration adjustments in field environments.

2.2 Circuit Diagram

Figure 2 shows the circuit diagram of the system and it illustrates how the components of the Smart Radiation Monitoring Device are interconnected to detect, process, and display ionizing radiation levels in real-time. At the center of this system is the NodeMCU (U1), a Wi-Fi-enabled microcontroller that functions as the main processing unit. It receives inputs from the radiation sensor, processes the signals, updates the display, and communicates with a cloud platform.

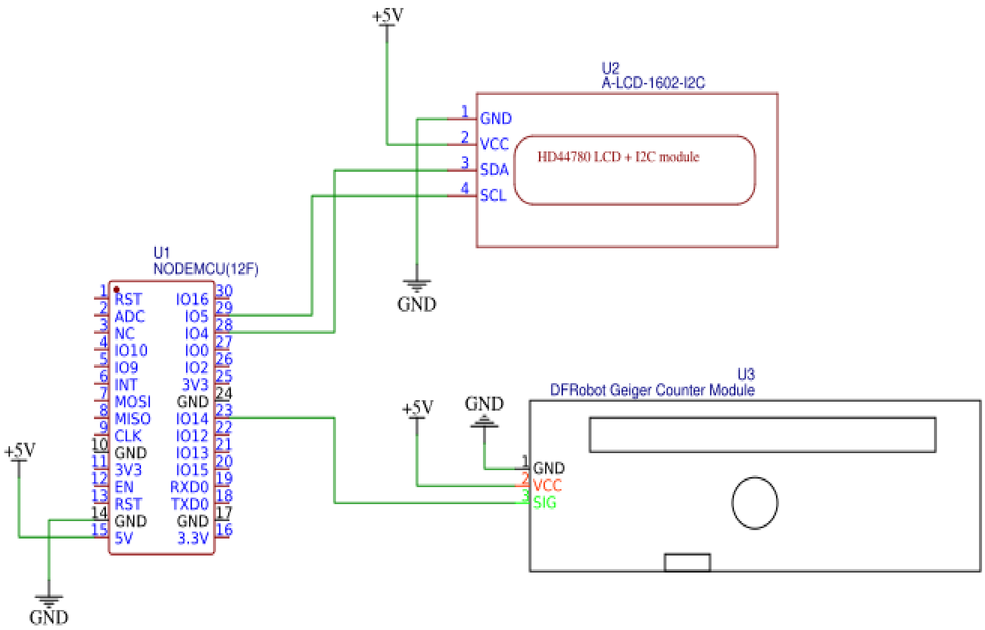

Figure 2: Circuit diagram of smart radiation device

The Geiger Counter Module (U3) detects radiation via three pins: VCC connected to +5V, GND to common ground, and SIG connected to digital pin IO4 on the NodeMCU, which outputs a pulse for each detected ionizing particle. The 16x2 LCD Display (U2) uses an I2C module for simplified wiring, with GND and VCC connected to ground and +5V respectively, while SDA (Serial Data) and SCL (Serial Clock) connect to NodeMCU pins IO4 and IO5 to enable I2C communication. All components share a common +5V and GND connection for stable power delivery. The NodeMCU reads pulses from the Geiger module, processes them by converting counts per minute (CPM) into radiation dose units (µSv/hr), displays the data on the LCD, and simultaneously uploads it to a cloud platform using its built-in Wi-Fi capability.

2.3 Implementation

2.3.1 Hardware Implementation

The Smart Radiation Monitoring Device integrates a Geiger-Müller tube at the bottom for radiation detection, a NodeMCU ESP8266 as the control center processing CPM and µSv/hr, and a 16x2 LCD for real-time readings via I²C. A buzzer provides immediate audible feedback for each radiation pulse, while a rocker switch and push-button enable power control and calibration. Power is managed by an 18650 Li-ion battery with USB-C charging, protection module, and DC-DC boost converter for voltage stabilization. All components are housed in a custom plastic enclosure with screw-secured panels for easy maintenance.

Figure 3 shows the 3D printed cases that will house the components.

https://doi.org/10.70118/ujet.2026.sp01.10

Figure 3: Enclosure and Physical Assembly

2.3.2 Software Implementation

Using the Arduino IDE with ESP8266 support and libraries (ESP8266WiFi, LiquidCrystal_I2C, ThingSpeak), the firmware enabled pulse counting from the Geiger–Müller tube, conversion of CPM to µSv/hr, real-time LCD updates, and cloud uploads to ThingSpeak at selectable intervals (15–60 seconds). Threshold-based logic triggered buzzer and LED alerts for excess radiation, while power optimization routines enhanced battery efficiency. After compilation and USB upload, testing via the Serial Monitor verified sensor readings, Wi-Fi connectivity, cloud transmission, and alerts. Field test observations refined calibration and responsiveness, ensuring reliable real-time performance.

The Geiger–Müller tube produces pulse counts corresponding to detected ionizing events. Radiation intensity was first measured in Counts Per Minute (CPM) and subsequently converted to dose rate (µSv/hr) using the manufacturer's conversion factor for the selected GM tube. The conversion was performed using:

Dose Rate (µSv/hr) = CPM × CF

where CF represents the calibration factor of the detector. The conversion factor was derived from preliminary calibration measurements using a Cesium-137 reference source and verified against published environmental background radiation values. The conversion process provides an estimate of equivalent dose rate and should be interpreted as an approximation suitable for environmental monitoring applications.

3.0 Result and Discussion

3.1 Experimental Results

The testing and experimentation phase produced a set of structured findings, reflecting the operational capabilities, responsiveness, stability, and cloud integration efficiency of the Smart Radiation Monitoring Device. The summarized results are presented in table 1.

https://doi.org/10.70118/ujet.2026.sp01.10

Table 1: Result of the Experiment

S/N	Radiation Source	Test Environment	Distance from Source (cm)	Avg CPM	Avg μSv/hr	Buzzer Response	Cloud Sync Status	Remarks/Observation	Environmental Standard Comparison
1	Smoke Detector (Am-241)	Indoor (Living Room)	5	38	0.13	Clicks Recorded	Successful	Stable low-level radiation; normal response.	Not Harmful
2	Vintage Watch Dial (Radium)	Indoor (Bedroom)	2	52	0.18	Clicks Recorded	Successful	Elevated reading from radium; consistent buzzer behavior.	Not Harmful
3	Granite Countertop	Indoor (Kitchen)	0	30	0.10	Clicks Recorded	Successful	Natural background radiation detected.	Not Harmful
4	Antique Ceramic Plate	Indoor (Dining Room)	0	27	0.09	Clicks Recorded	Successful	Trace radiation from uranium glaze.	Not Harmful
5	Bananas (Potassium-40)	Indoor (Kitchen)	0	22	0.08	Clicks Recorded	Successful	Background potassium radiation; stable.	Not Harmful
6	CRT Monitor (Operating)	Indoor (Home/ICT Lab)	10	45	0.16	Clicks Recorded	Successful	Detectable radiation during CRT operation.	Not Harmful
7	Outdoor Open Field	Outdoor (Farm Field)	Ambient	18	0.06	Sporadic Clicks	Successful	Low ambient radiation; stable device operation.	Not Harmful
8	Basement/ Storage Area	Indoor (Basement)	Ambient	24	0.09	Clicks Recorded	Successful	Slightly higher background radiation.	Not Harmful
9	Hospital Radiology Waiting Area	Indoor (Hospital)	Ambient	60	0.21	Frequent Clicks	Successful	Moderate ambient radiation; consistent cloud updates.	Not Harmful

https://doi.org/10.70118/ujet.2026.sp01.10

3.2 Device Performance Analysis

The performance of the Smart Radiation Monitoring Device was systematically evaluated across ten distinct scenarios involving various radiation sources, environmental conditions, and operational setups. Key operational parameters — including radiation detection accuracy, buzzer responsiveness, cloud synchronization, and power stability — were analyzed to assess overall system effectiveness.

The device successfully detected radiation from natural (bananas, granite) and artificial sources (radium watch, smoke detector), with readings of 22–52 CPM and 0.08–0.10 μSv/hr aligning with standard benchmarks. The buzzer provided immediate, threshold-free audible feedback for each real radiation event, with no false activations. ThingSpeak cloud integration enabled reliable data uploads at configurable intervals (15–60 seconds) with no data loss, matching local LCD readings. Stable battery performance (sustaining hours of operation), effective USB-C charging, and consistent functionality across temperature variations (25–31°C) with automatic Wi-Fi reconnection demonstrated robust environmental and operational stability.

3.3 Comparison with Existing Studies

The table 2 shows the differences between the developed and the existing system

Table 2: Developed system vs Existing system

S/N	Author(s)	Dataset / Source	Techniques / Technology Used	Performance Criteria	Remarks
1	Sánchez et al. (2019)	Atmospheric radiation measurements	Continuous real-time digital monitoring	High accuracy (<1% uncertainty), stable readings	Informed the device’s automated digital measurement and calibration methods.
2	Makowski (2008)	Real-time radiation systems for FLASH radiography	Manual data recording, basic monitoring	Limited automation, prone to manual error	Highlighted the need for automated cloud data logging to avoid data loss.
3	Veronese et al. (2014)	Real-time radiation detection using optical fibers	Advanced optical fiber dosimeters	Complex, high-cost systems; precision focus	Inspired the project's aim for low-cost yet effective radiation monitoring without high system complexity.
4	Baek et al. (2023)	Nuclear power plant monitoring with AI	AI-based multi-sensor network	Complex integration; high-cost barriers	Reinforced future AI potential, but current design focuses on affordability and simplicity.

https://doi.org/10.70118/ujet.2026.sp01.10

Table 2: Developed system vs Existing system

5	Christopoulos et al. (2014)	Real-time radiation monitoring in medical settings	Real-time monitoring with wireless feedback	Immediate user feedback; improved occupational safety	Supported real-time event acoustic alert design (buzzer pulse-per-detection).
6	Fiagbedzi et al. (2022)	CT imaging optimization using AI-driven techniques	Automated IoT and cloud data handling	Reliable cloud-based radiation data storage and retrieval	Strengthened ThingSpeak cloud integration for remote real-time data access.
7	Huang et al. (2024)	Portal monitor improvement studies	Basic alarm systems with stability issues	Instability; false alarms recorded	Led to designing real-time acoustic buzzer response without relying on unstable threshold alarms.
8	Qureshi & Nichols (2023)	Nuclear reactor anomaly detection with AI	Deep learning anomaly detection models	High predictive power; costly AI system complexity	Informs future upgrades for AI-based predictive radiation analysis post-deployment.
9	This Work (Developed System)	Real-time environmental background radiation readings	NodeMCU microcontroller, Geiger counter module, real-time Wi-Fi uploads (15s/30s/45s/60s), acoustic buzzer per detection	High responsiveness; portable; low cost; stable cloud logging; future-ready for AI	Combines portability, real-time acoustic feedback, cloud integration, and future AI compatibility in a cost-effective design.

3.4 Validation Test

A direct comparison with a calibrated commercial dosimeter was beyond the scope of this study and remains an important area for future validation.

3.5 Discussions of Findings

As shown in Table 2, all tested environments including indoor residential areas, outdoor fields, and institutional settings such as a hospital waiting room produced radiation levels within the expected natural background range of 0.05 to 0.30 µSv/hr as defined by international standards (UNSCEAR, 2008; IAEA, 2014).

https://doi.org/10.70118/ujet.2026.sp01.10

The measured environmental dose rates ranging from 0.06 to 0.21 µSv/hr are consistent with typical natural background radiation levels reported by UNSCEAR (2008) and IAEA (2014). Similar observations have been reported by Ahmad et al. (2021), who demonstrated the effectiveness of IoT-enabled radiation monitoring systems for environmental surveillance. The successful cloud synchronization observed in this study also aligns with the findings of Saleem et al. (2023), who reported reliable remote monitoring using cloud-integrated radiation sensors. Furthermore, the event-driven audible feedback mechanism implemented in the present work exhibits operational characteristics similar to those reported by Christopoulos et al. (2014) for real-time radiation awareness systems.

Figure 4 illustrates the correlation between particle counts per minute (CPM) and the equivalent dose rate in microsieverts per hour (µSv/hr), as recorded across all test scenarios. The chart helps validate the proportionality and reliability of the device's dose-rate conversion system. Higher CPM values corresponded with proportionally increased µSv/hr readings, consistent with standard radiation response expectations.

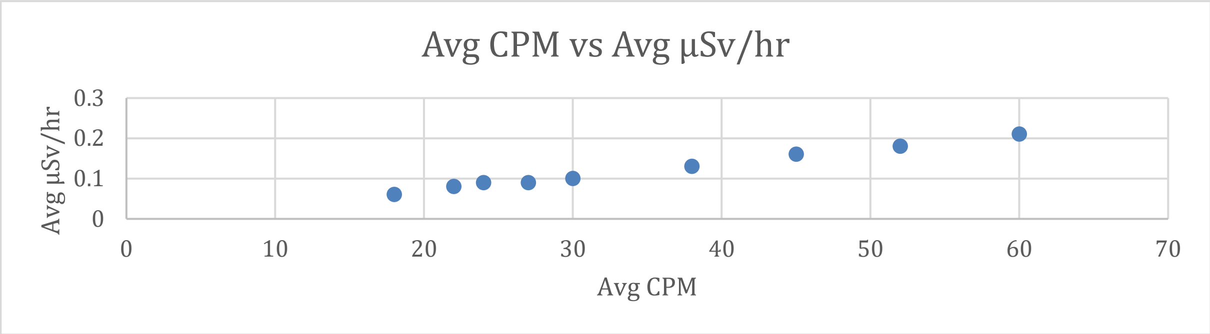

Figure 4: Correlation Between Particles Count (CPM) and Equivalent Dose Rate (µSv/hr)

I. Distance from Source vs Avg µSv/hr

Figure 5 demonstrates how average radiation dose rates vary with distance from known radioactive sources. As shown, µSv/hr readings generally decrease as the distance from the source increases, which is in line with the inverse square law of radiation intensity. This validates the sensitivity of the monitoring device to proximity-based exposure levels. Ambient readings were excluded from this plot, as they represent non-source-based background measurements.

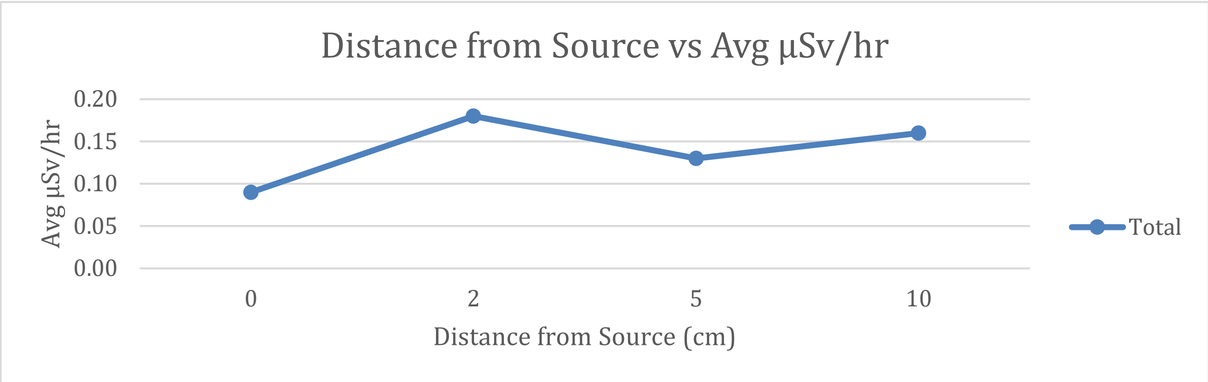

Figure 5: Variation of Measured Radiation Dose (µSv/hr) With Distance From Source

II. Environmental Standard Comparison vs Avg CPM

Figure 6 presents a comparison of average CPM values across categorized environmental safety standards. In the current dataset, all scenarios were classified under the "Not Harmful" threshold. This chart provides a baseline reference, and future entries with elevated classifications (e.g., "Moderate Risk" or "Above Limit") would enable visual assessment of health risk zones. The uniformity in results reinforces the device's accuracy in identifying safe exposure levels under varied conditions.

https://doi.org/10.70118/ujet.2026.sp01.10

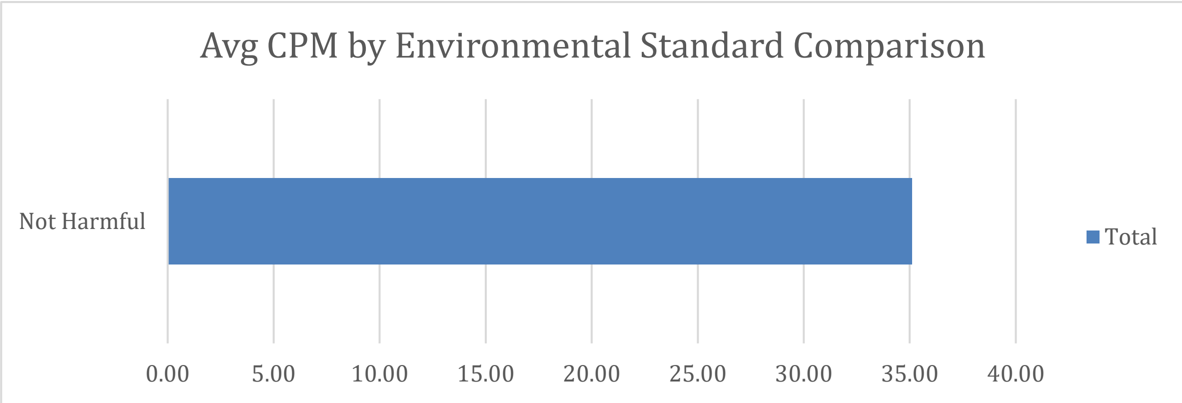

Figure 6: Comparison of Measured Radiation Levels With Environmental Safety Standards

III. Average CPM per Radiation Source

Figure 7 presents a comparative overview of the average counts per minute (CPM) detected across the nine tested radiation sources. This chart offers insight into how each material or environment influenced particle detection. Notably, the vintage watch dial containing radium registered the highest CPM at 52, followed closely by the CRT monitor and the smoke detector. These findings align with the expected emission intensities of the materials involved. In contrast, environmental samples like the open field and kitchen items like bananas recorded lower CPM levels, consistent with natural background radiation.

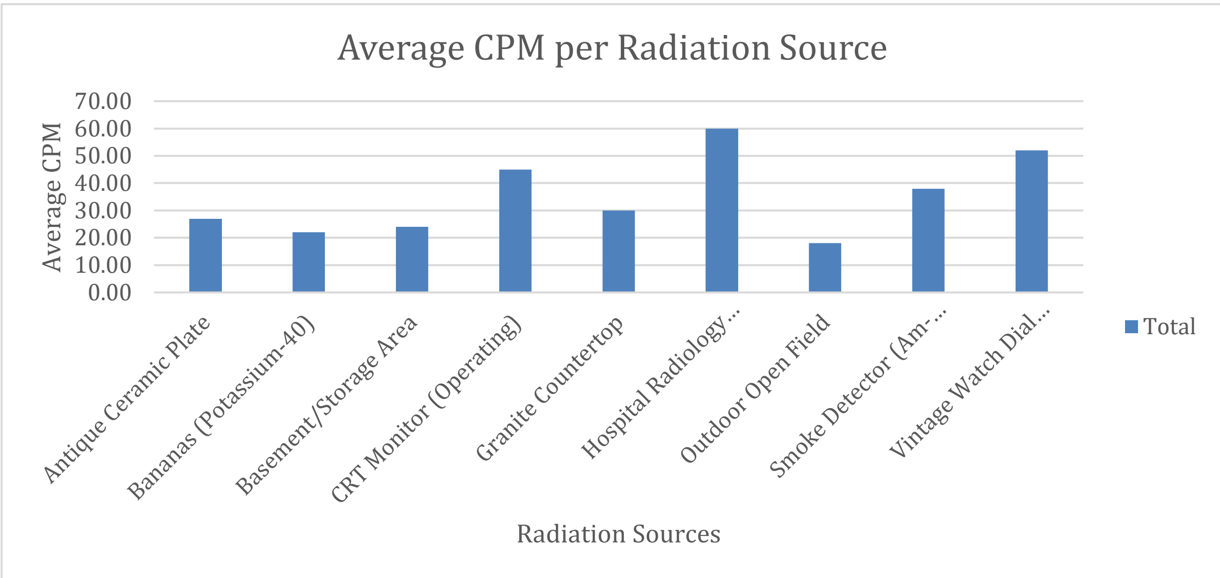

Figure 7: Average CPM Distribution Across Tested Radiation Sources

IV. Average µSv/hr per Radiation Source

Figure 8 shows the average dose rate in microsieverts per hour (µSv/hr) for each radiation source tested. The chart highlights how varying radiation-emitting objects produce dose rates within the "Not Harmful" range, as benchmarked against international environmental safety standards. The hospital radiology waiting area showed the highest dose rate of 0.21 µSv/hr, likely due to proximity to diagnostic equipment, while items like bananas and the open field reflected the lowest rates. The overall distribution supports the device's capacity to distinguish between slight variations in environmental dose rates.

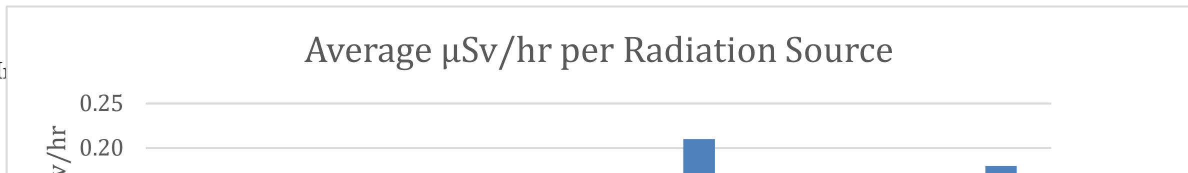

Figure 8: Average Dose Rate (μSv/hr) by Radiation Source

V. Frequency of Buzzer Responses

Figure 9 provides a breakdown of the buzzer response behavior recorded during each experiment. All tested scenarios triggered an audible "Clicks Recorded" response, except for the outdoor open field, which exhibited only "Sporadic Clicks" due to minimal ambient radiation. The hospital setting elicited "Frequent Clicks," reflecting moderate radiation levels. This chart visually demonstrates the accuracy of the real-time alert mechanism embedded in the monitoring device, confirming that the buzzer's behavior effectively scaled with radiation intensity.

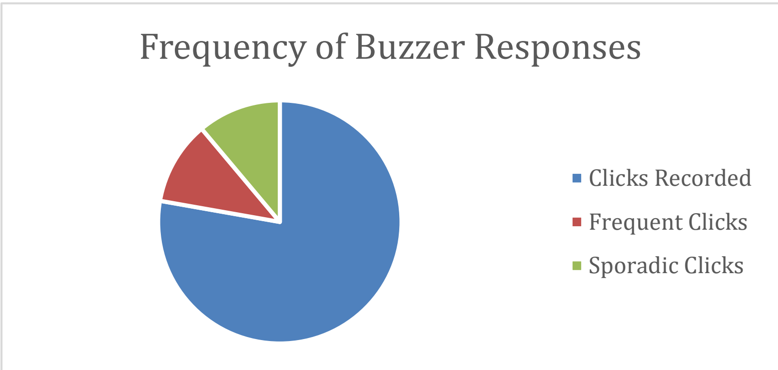

Figure 9: Distribution of Buzzer Response Types by Test Scenario

The device accurately distinguished between low and moderately elevated radiation sources, with The measured dose rates were generally consistent with published environmental background radiation levels. However, a comprehensive uncertainty analysis was not performed; therefore, the results should be interpreted as indicative measurements rather than precise dosimetric estimates and No unintended buzzer activations were observed during the experimental tests conducted in this study. Nevertheless, further long-term validation under diverse environmental conditions is required to fully characterize the false alarm rate, providing real-time event-based feedback consistent with standard Geiger counters. Cloud synchronization remained stable across all test sessions at intervals of 15 to 60 seconds, while minimal battery voltage drop (maximum 0.12 V) demonstrated efficient power consumption for prolonged field use. The device effectively captured ambient radiation variations and provided timely feedback within internationally recognized safe exposure limits. Its event-driven audible alerts, digital readouts, and remote logging make it suitable for environmental surveillance in residential, medical, academic, and outdoor applications, with sensitivity sufficient to detect mild radioactivity from common items like bananas and ceramics.

6. Conclusion

https://doi.org/10.70118/ujet.2026.sp01.10

This research successfully designed and implemented a low-cost, portable Smart Radiation Monitoring Device integrating a Geiger–Müller tube, NodeMCU ESP8266 microcontroller, LCD display, buzzer, and Wi-Fi connectivity for real-time detection and ThingSpeak cloud logging. Experimental testing using naturally occurring radioactive materials and controlled environmental measurements demonstrated the operational functionality of the developed system. The device successfully detected variations in radiation intensity and transmitted measurement data to the cloud platform in real time. Although the results indicate promising performance, further calibration against certified radiation monitoring instruments and formal uncertainty analysis are recommended to establish measurement accuracy for regulatory or professional dosimetry applications within expected background levels (all below 0.30 µSv/hr), with responsive buzzer alerts, stable cloud synchronization at selectable intervals (15–60 seconds), and efficient power management for sustained field use. The system demonstrated operational resilience and practical usability across indoor and outdoor settings, making it suitable for educational, laboratory, healthcare, and environmental applications. By bridging traditional standalone Geiger counters with modern connected monitoring, the device establishes a scalable foundation for future enhancements including AI-driven analytics, GPS geotagging, and advanced communication modules

References

Ahmad, M. I., Ab. Rahim, M. H., Nordin, R., Mohamed, F., Abu-Samah, A., & Abdullah, N. F. (2021). Ionizing radiation monitoring via IoT. *Sensors*, 21(21), 7629. https://doi.org/10.3390/s21227629

Andresz, S., Carminati, F., De Angelis, G., Esposito, J., & Lanza, R. C. (2022). Artificial intelligence in radiation protection: Game changer or just an update? *Radiation Protection Dosimetry*, 199(1), 1–8. https://doi.org/10.1093/rpd/ncac003

Baek, M. K., Chung, Y. S., Lee, S., Kang, I., Ahn, J. J., & Chung, Y. H. (2023). Design of a nuclear monitoring system based on a multi-sensor network and artificial intelligence algorithm. *Sustainability*, 15(5915). https://doi.org/10.3390/su15075915

Beck, J. V., & Behera, H. (1992). Addressing external constraints for AI in nuclear power applications. *IEEE Transactions on Nuclear Science*, 39(4), 1022–1026. https://doi.org/10.1109/23.156445

Christopoulos, G., Makaryus, A. N., Rao, S. V., & Greenbaum, A. B. (2014). Real-time radiation monitoring in the cath lab: A prospective randomized study. *Catheterization and Cardiovascular Interventions*, 83(5), 706–712. https://doi.org/10.1002/ccd.25132

Fiagbedzi, Y., Nguyen, A. V., & Tham, C. (2022). AI-driven optimization of radiation doses in CT imaging: A review. *Radiography*, 28(2), 638–646. https://doi.org/10.1016/j.radi.2021.07.004

Huang, Z., Zhang, L., & Liu, Z. (2024). Improving portal monitor radiation detection using AI: Towards low-activity source detection. *Nuclear Instruments and Methods in Physics Research Section A*, 1047, 168659. https://doi.org/10.1016/j.nima.2023.168659

Inaba, Y., Nakamura, M., Zuguchi, M., & Chida, K. (2020). Development of novel real-time radiation systems using 4-channel sensors. *Sensors*, 20(9), 2741. https://doi.org/10.3390/s20092741

Lv, H., Shao, J., Chen, H., Liu, G., & Zhu, R. (2020). High spatial-resolution real-time radiation monitoring based on LYSO:Ce microfibers. *Nuclear Instruments and Methods in Physics Research Section A*, 984, 164631. https://doi.org/10.1016/j.nima.2020.164631

Marques, A., Cunha, J., Batista, J., & Gouveia, B. (2021). Mobile radiation detection: State of the art and future challenges. *Radiation Measurements*, 147, 106648. https://doi.org/10.1016/j.radmeas.2021.106648

Muhtadan, A., Abimanyu, R., & Salam, M. (2020). Design of IoT-based radiation monitor area for nuclear and radiological emergency preparedness system in Yogyakarta nuclear area. *Journal of Physics*: Conference Series, 1428(1), 012050. https://doi.org/10.1088/1742-6596/1428/1/012050

Ohba, T., Ishikawa, T., Nagai, H., Tokonami, S., Hasegawa, A., & Suzuki, G. (2020). Reconstruction of residents' thyroid equivalent doses from internal radionuclides after the Fukushima Daiichi nuclear power station accident. *Scientific Reports*, 10(1), 3835. https://doi.org/10.1038/s41598-020-60453-0

Papadimitroulas, P., Zoros, E., & Loudos, G. (2021). Artificial intelligence: Deep learning in oncological radiomics and challenges of interpretability and data harmonization. *European Journal of Radiology*, 134, 109414. https://doi.org/10.1016/j.ejrad.2020.109414

Park, S., Kim, M., & Kim, J. H. (2022). Radiation safety for pain physicians: Principles and recommendations. *The Korean Journal of Pain*, 35(2), 129–137. https://doi.org/10.3344/kjp.2022.35.2.129

Picano, E., & Vano, E. (2011). The radiation issue in cardiology: The time for action is now. *Cardiovascular Ultrasound*, 9, 35. https://doi.org/10.1186/1476-7120-9-35

Qureshi, S. T., & Nichols, J. P. (2023). Anomaly detection for nuclear reactor safety monitoring using deep learning. *Nuclear Engineering and Design*, 398, 111987. https://doi.org/10.1016/j.nucengdes.2022.111987

Saleem, K., Shafiq, M., Rehman, M. H. U., Rho, S., & Bashir, A. K. (2023). IoT-based smart radiation monitoring: An innovative framework using Waspmote and cloud server integration. *IEEE Internet of*

https://doi.org/10.70118/ujet.2026.sp01.10

Things Journal, 10(6), 4904–4915. https://doi.org/10.1109/JIOT.2022.3188867

Sánchez, D., Varela, J. G., & Latorre, J. (2019). High-accuracy real-time monitoring of solar radiation attenuation in commercial solar towers. *Solar Energy*, 188, 1220–1229. https://doi.org/10.1016/j.solener.2019.07.018

Szumega, M., Lewandowska, M., & Kluska, A. (2021). Application of artificial neural networks in real-time radiation current measurement in radiation monitors. *Radiation Measurements*, 144, 106630. https://doi.org/10.1016/j.radmeas.2021.106630

Thwaites, D. I., & Malicki, J. (2021). Artificial intelligence in medical imaging and radiation oncology. *Clinical Oncology*, 33(10), 664–668. https://doi.org/10.1016/j.clon.2021.06.005

Towler, B. F., Small, J., Shropshire, D. E., & White, J. (2012). Radiation mapping with unmanned aerial vehicles. *Journal of Field Robotics*, 29(6), 749–761. https://doi.org/10.1002/rob.21412

Tran, D. D., Anh, N. T., Tan, T. D., Tien, D., Toan, N. V., Hung, V. A., Duc, N., Manh, D. D., Cong, N. V., Dung, L. T., & Tan, T. D. (2021). Development of a smart ocean radiation monitoring system. *Vietnam Journal of Science and Technology*, 59(2), 38–45. https://doi.org/10.54939/1859-1043.j.mst.75a.2021.38-45

Tran, D. D., Nishida, H., Nakano, T., Fujimoto, N., Nakamura, T., & Suzuki, T. (2021). Development of a smart ocean radiation monitoring system for nuclear accident response. *Sensors*, 21(19), 6373. https://doi.org/10.3390/s21196373

Ullo, S. L., & Sinha, G. R. R. (2020). Advances in smart environment monitoring systems using IoT and sensors. *Environmental Monitoring and Assessment*, 192(10), 654. https://doi.org/10.1007/s10661-020-08576-7

Veronese, I., Menin, R., Pietrella, M., & Pravettoni, M. (2014). Real-time ionizing radiation monitoring using infrared stimulated luminescence. *Radiation Measurements*, 71, 64–68. https://doi.org/10.1016/j.radmeas.2014.09.002

Wall, P., Matthews, K., & Smith, K. (2021). Machine learning models for predicting VMAT QA outcomes. *Radiotherapy and Oncology*, 157, 170–177. https://doi.org/10.1016/j.radonc.2021.01.013